Title

Seismic monitoring of a small CO2 injection using a multi-well DAS array: Operations and initial results of Stage 3 of the CO2CRC Otway project

Authors

Pevzner, Roman

Isaenkov, Roman

Yavuz, Sinem

et al.

Publication Date

2021-09-01

DOI

10.1016/j.ijggc.2021.103437

Peer reviewed

Seismic monitoring of a small CO_2 injection using a multi-well DAS array: operations and initial results of Stage 3 of the CO2CRC Otway project

Roman Pevzner[1,2], Roman Isaenkov[1,2], Sinem Yavuz[1,2], Alexey Yurikov[1,2], Konstantin Tertyshnikov[1,2], Pavel Shashkin[1,2], Boris Gurevich[1,2], Julia Correa[3], Stanislav Glubokovskikh[1,2,3], Todd Wood[3], Barry Freifeld[4], Paul Barraclough[2]

[1]Curtin University, Centre for Exploration Geophysics, GPO Box U1987, Perth, WA, Australia

[2] CO2CRC, 11 – 15 Argyle Place South, Carlton, VIC, 3053, Australia

[3] Lawrence Berkeley National Laboratory, 1 Cyclotron Road, MS 74R-316C, Berkeley, CA, USA, 94720

[4] Class VI Solutions, Inc., 711 Jean St., Oakland, CA, USA, 94610

Corresponding author:

Sinem Yavuz Sinem.Yavuz@curtin.edu.au

Postal address:

Curtin University, GPO Box U1987, Perth, WA, Australia

Abstract

Active time-lapse seismic is widely employed for monitoring CO_2 geosequestration due to its ability to track the distribution of fluids in space and time. However, standard 4D seismic monitoring suffers from several challenges, including high cost, disruption to other land uses, and, consequently, relatively large intervals between monitor surveys. Some of these challenges can be mitigated using permanently installed sources and receivers. Such an approach was tested at the CO2CRC Otway site by continuous offset VSP monitoring of 15,000 t of supercritical CO_2 injected into an aquifer 1,500 m

deep with nine permanent seismic sources (surface orbital vibrators or SOVs) and five downhole fibre-optic receivers. This continuous monitoring is complemented by multi-well 4D VSP using a mobile vibroseis source and the same DAS receivers, which included one baseline and two monitor surveys after injection of 4,000 and 12,000 t of CO_2. The continuous DAS-SOV monitoring detected an abrupt increase of travel times below the injection interval on the second day of injection (after injection of 300 t of CO_2) and tracked the growth of the areal CO_2 plume by mapping changes of reflection amplitudes. The plume is also detected by time-lapse changes of reflection amplitudes in multi-well 4D VSPs. The plume images obtained from continuous offset VSP and 4D VSP are broadly consistent with each other but with some differences due to differences in illumination, lateral variations of velocities and seismic anisotropy. These differences also serve as a measure of uncertainty of 4D VSP images.

1 Introduction

Active time-lapse seismic is widely employed for monitoring CO_2 geosequestration due to its ability to track the distribution of CO_2 in space and time with better spatial resolution than any other remote sensing technique (Johnston, 2013; Lumley, 2010; Mathieson et al., 2010). Seismic monitoring has been successfully applied for the monitoring of industrial-scale injections as well as small-scale research projects (Ajayi et al., 2019).

Yet standard surface 4D seismic has several specific problems which limit the application of the method. These include relatively high cost (Mathieson et al., 2011) and disruption to other users of land or marine resources. Also, because of these challenges, 3D monitor surveys are acquired months or years apart and take several months to process and derive an interpretable result. Thus, 4D seismic monitoring has a relatively sparse temporal sampling and provides an outdated image of the subsurface. A rare example where land 4D seismic was acquired with a dense temporal sampling of ~1 month between the surveys was reported by Jervis et al. (2018); however, this required a permanently deployed receiver array.

Disturbance to the environment can be greatly reduced by using borehole seismic methods, which can also improve data quality and repeatability. Attempts to use vertical seismic profiling (VSP) for monitoring were reported from various CO_2 geosequestration projects. These include time-lapse VSP acquired with conventional geophone tools, such as in the Decatur Project (Bauer et al., 2019; Couëslan et al., 2013). The use of shallow boreholes instrumented with seismic sensors has been suggested as a cost-effective strategy for CO_2 injection (Majer et al., 2006) in Weyburn Field. More recently, the rapid development of distributed acoustic sensing (DAS) (Hartog, 2017) boosted the use of borehole seismic for monitoring, with many current projects trialling or relying on this technology (Bacci et al., 2017; Daley et al., 2013; Michael et al., 2020; White et al., 2019). Most of these experiments use 3D VSP or walk-away geometry with receivers deployed in a single well, which provides limited spatial coverage. Recently Mateeva et al. (2017) showed that 4D VSP in multi-well configuration increases the spatial coverage of reservoir production monitoring. However, 3D VSP surveys can still only be acquired at relatively sparse intervals due to the prohibitively high cost of frequent surveys.

Higher temporal sampling can be achieved by employing a permanent seismic source paired to a permanently (or semi-permanently) installed receiver array. Piezoceramic vibrators (Zwartjes et al., 2015) were successfully applied to steam injection monitoring. A variety of permanent sources were tested for CO_2 geosequestration monitoring. Most of the trials have focused on the performance of the sources rather than on actual injection monitoring. A linear electromagnetic vibrator on the surface was trialled at Ketzin (Arts et al., 2013). A large eccentric vibrator was deployed at the Aquistore site (Nakatsukasa et al., 2016); however, seasonal near-surface variations precluded the use of the data to monitor the injection (Ikeda et al., 2017). Dual-motor permanent eccentric sources were tested at the CaMI project (Andersen, 2019; Spackman, 2019). A semi-permanent weight drop source was used to attempt detection of the CO_2 plume edge in the Bell Creek CO_2 EOR project (Burnison et al., 2017); this was followed by deployment of another single-motor eccentric surface orbital vibrator

(SOV) (Barajas-Olalde et al., 2020). None of these examples provided a spatial image of the CO_2 plume or estimated the detectability limits.

The Stage 3 of the CO2CRC Otway project aims to test downhole geophysical monitoring techniques for continuous or on-demand information about the evolution of a CO_2 plume in the subsurface (Jenkins et al., 2017). The design of the injection experiment is based upon the findings of previous stages of the Otway project, which includes seismic monitoring of a series of small-scale CO_2 injections into several subsurface formations at a dedicated site in the Australian state of Victoria.

In the Stage 1 of the CO2CRC Otway project, 65,000 tonnes of supercritical CO_2/CH_4 mixture (referred to simply as CO_2 below) was injected into a depleted methane gas reservoir at ~2 km depth using the dedicated CRC-1 well. Both surface and borehole 4D seismic were used to attempt to detect the plume and ensure the absence of leakage (Gurevich et al., 2014). The results showed higher repeatability of VSP data compared to surface seismic but no clear time-lapse response from the injection, as changes of elastic properties of the reservoir were too small due to the presence of residual methane gas.

Stage 2C of the project was focused on imaging a small-scale CO_2 injection into a saline aquifer at a depth of 1.5 km, known as the Paaratte formation. To this end, 15,000 t of CO_2 was injected through a new CRC-2 well, while CRC-1 was converted to a monitoring well. The seismic monitoring was done using 4D surface seismic with a dedicated array of geophones buried 4 m below the surface, 4D VSP with geophones and several time-lapse offset VSPs. Each of these methods was successful in detecting as little as 5,000 t and monitoring the evolution of the plume (Pevzner et al., 2020c). The Stage 2C injection was also used to trail the performance of DAS (Correa, 2018; Daley et al., 2013) and asynchronous SOVs (Freifeld et al., 2016). The DAS trials included several DAS interrogators (Silixa iDAS v1, v2 and v3 and Fotech Helios Theta) and various techniques for deploying sensing cables, both downhole and trenched.

The Stage 3 injection parameters (total volume, target formation and season) are identical to those of Stage 2C; however, the injector well, CRC-3, is located ~600 m down dip from CRC-2.

The seismic monitoring program of Stage 3 is focusing on the development of an automated continuous downhole monitoring system using five wells instrumented with fibre-optic sensing cables (including DAS) and nine permanently deployed SOVs. Continuous time-lapse VSP acquired with SOVs is designed to provide information about day-by-day plume evolution in near-real-time. Key technology components include complete automation of the data processing and remote operation of both source and receiver arrays.

To validate images obtained from SOV operation, the program is complemented with 4D VSP acquired using the same fibre-optic sensing cables and conventional vibroseis sources.

In this paper, we describe the overall monitoring strategy and share the initial results.

2 Seismic monitoring program and operations

The seismic monitoring program of Stage 3 of the CO2CRC Otway Project consist of the following components:

1. Drilling and completion of five deep wells instrumented with fibre-optic cables: one injector and four dedicated monitoring wells
2. Deployment of an array of nine surface orbital vibrators (SOVs) used as continuous seismic sources.
3. Development and deployment of hardware and software for interfacing the receiver array with continuous sources and on-site data processing facilities
4. Acquisition of the 4D VSP survey comprising of a baseline and two monitor surveys using conventional vibroseis.
5. Continuous monitoring using DAS/SOV array.

A simplified timeline of the operations linked to the seismic monitoring program is shown in Figure 1.

As the receiver array has been recording data continuously over 12 months (apart from several operational gaps), the acquired data can also be used for passive seismic imaging and analysis of induced seismicity.

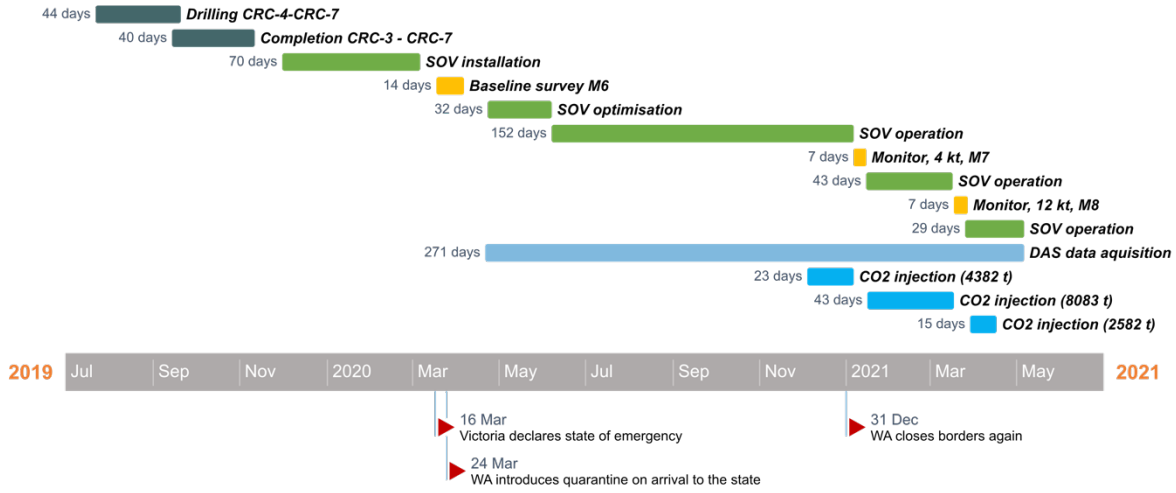

Figure 1. A simplified seismic monitoring timeline

2.1 Downhole instrumentation for seismic monitoring

CO2CRC Otway Project site has multiple wells equipped with fibre-optic cables. Figure 2 shows the location of the wells and surface infrastructure used in Stage 3 of the project.

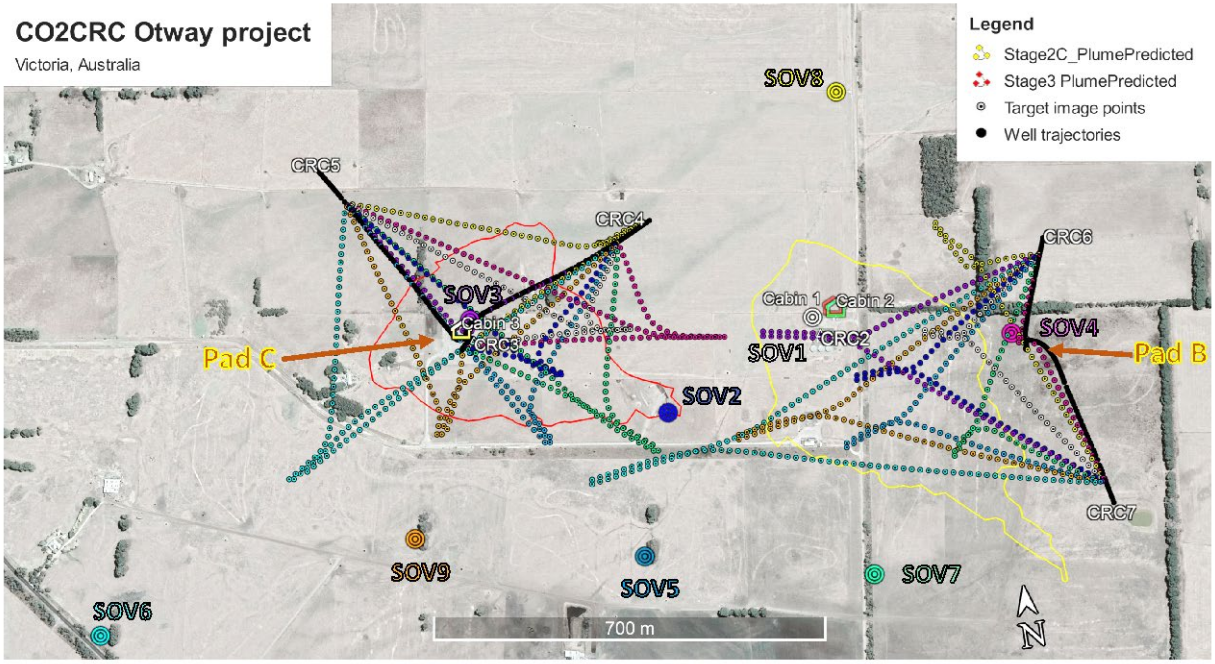

130 *Figure 2. Location map of wells and surface orbital vibrators (SOVs). Dotted lines show the projection*
131 *of specular reflection points at the target interval colour-coded by the corresponding SOV. Stage 2C*
132 *and Stage 3 predicted plume contours are simulated for 15,000 t CO_2 injection.*

133 The CRC-2 well was drilled in 2010 as a CO_2 injector for Stage 2 of the Otway Project and was
134 instrumented with a fibre-optic cable with a combination of single-mode (SMF) and multi-mode
135 (MMF) fibres deployed on production tubing (Daley et al., 2013).

136 CRC-3 is a vertical well drilled in 2017 used initially as an appraisal well and then completed as a CO_2
137 injector for Otway's Stage 3. Two fibre-optic cables were cemented behind the casing. One cable is
138 deployed to the total well depth (TD) and carried SMF, MMF, and a specialised SMF with increased
139 backscattering to enhance DAS sensitivity (Constellation fibre by Silixa, denoted EBS1). Another cable
140 carrying conventional SMF and MMF is deployed to a slightly shallower depth, just above the
141 perforation interval.

142 The dedicated monitoring wells (CRC-4, CRC-5, CRC-6 and CRC-7) were drilled, perforated and
143 completed in 2019. These four wells deviate with a maximum vertical inclination of 20-22 degrees.
144 Similar to CRC-3, each of these wells has two fibre-optic cables cemented behind the casing: one cable

145 with EBS1, SMF and MMF deployed to TD and another cable with a similar combination of fibres
146 (including one specialty fibre, EBS2 from another manufacturer supplied by Sercel) terminated above
147 the perforation zone.

148 The CRC-3 well was perforated in 2019 and was completed with production tubing with a fibre-optic
149 cable clamped to it. Finally, an extra fibre-optic cable was suspended in the CRC-4 well to test fibre
150 sensing in a tubing-less completion (Table 1).

151 *Table 1. Fibre-optic cables deployed in the wells (SMF – single-mode fibre, EBS1,2 – enhanced*
152 *backscatter fibres from different suppliers, EBS1 corresponds to Constellation, EBS2 was supplied by*
153 *Sercel, all cables also have multi-mode cores)*

Well	Cemented behind the casing	Clamped to production tubing	Suspended in the well
CRC-2	-	1 cable, SMF	-
CRC-3	2 cables, SMF	1 cable, SMF + EBS1	-
CRC-4	2 cables, SMF + EBS1 + EBS2	-	1 cable, SMF
CRC-5	2 cables, SMF + EBS1 + EBS2	-	-
CRC-6	2 cables, SMF + EBS1 + EBS2	-	-
CRC-7	2 cables, SMF + EBS1 + EBS2	-	-

154

155 All the wells drilled for Stage 3 were designed to be deeper than the perforation interval by at least
156 100 m. This was done to ensure the placement of seismic sensors underneath the perforation interval
157 to enable seismic monitoring using both reflected and transmitted waves.

158 In addition to the borehole receiver arrays, one km-long helically-wound fibre-optic cable with SMF
159 and a Constellation fibre was deployed in the trench connecting two drill pads for CRC-3, CRC-4 and
160 CRC-5 wells (Pad C) and CRC-6 and CRC-7 (Pad B).

2.2 DAS Monitoring of drilling and completion

During the drilling of the new wells, one DAS recording unit (iDASv3 by Silixa Ltd) with a gauge length of 10 m was deployed in Cabin 2 (see Figure 2). This unit was connected to the CRC-2 well (SMF fibre) for continuous acquisition commencing January 2019. On July 27, a temporary ~700 m long surface cable was installed connecting Cabin 2 to Pad B, and the DAS unit was reconnected to the Constellation fibre in CRC-3. At that time, drilling of the CRC-4 well reached ~1 km MD, and thus DAS was able to record data during the remainder of the drilling from close vicinity. By August 14, CRC-4 had been cased, and the CRC-3 and CRC-4 cables were connected to the same interrogator and recorded the final stages of CRC-5 drilling using these two downhole cables. The same configuration was used to monitor the drilling of CRC-6 and CRC-7. Initial data analysis shows both P and S wave energy emitted by the drill bit (Pevzner et al., 2020a; Qin et al., 2020).

The DAS cable configuration described above has substantial redundancy, designed to ensure that even if the main casing conveying fibre-optic cables deployed to the total depth sustains damage during installation or perforations, at least some SMF fibres in each well would still be intact and available for data acquisition during and after CO_2 injection. As such, using DAS to monitor perforations was important to validate cable integrity and signal quality. All five CRC-3 – CRC-7 wells were perforated in September 2019. In each well, two directional shots were fired. Schlumberger's PURE perforation system, which creates a transient underbalance was used to provide clean perforation clusters in CRC-3 and CRC-4.

During the perforations, we used two interrogators, Silixa iDAS v3 with 10 m gauge length connected to Constellation fibre in one or two wells (depending on availability) and Silixa iDAS v2 with 3 m gauge length. This unit was connected to the well that is being perforated (integrity monitoring) while the other unit (Silixa iDAS v3) recording the far-field signature of the shot.

Given the known position of the perforation shots, DAS data acquired during perforation can be used to calibrate the seismic velocity model accurately. Having an accurate velocity model is critical to estimate the location of any fluid-induced seismic events that could be triggered during the injection.

During the completion stage, we also tested data acquisition using different ways of downhole DAS deployment, including casing- and tubing-conveyed cables in CRC-3 and casing-conveyed and suspended cables in CRC-4. The results are presented in Pevzner et al. (2020b).

2.3 Design and deployment of the permanent sources array.

The SOVs deployed at the Otway site are of two types. SOV1 and SOV2 are 1st-generation SOV's deployed during the Stage 2C (Freifeld et al., 2016). Each of those has two motors with eccentric weights; however, only one motor can operate at a time, and switching between the motors requires the physical presence of the operator on-site (Correa et al., 2018a). Large motors can reach a frequency of 80 Hz with 10 t peak force, while the smaller motor can reach frequencies exceeding 100 Hz but with significantly lower power (2.5 t). The location of these vibrators was driven by Stage 2C requirements to optimise imaging CO_2 near the CRC-2 well.

SOV3-SOV9 are 2nd generation SOVs deployed specifically for the Stage 3 monitoring program. These SOVs have two motors with eccentric weights, but, unlike the older version, they can operate the motors concurrently. Location of the sources (Figure 2) was selected such that the location of the specular reflection points (dotted lines on the figure) would densely cover the predicted Stage 3 plume (yellow contour) and pre-existing Stage 2C plume (red contour). Note that the evolution of the Stage 3 plume can be mapped even if it deviates from the reservoir simulations as specular reflection points encircle CRC-3 along numerous azimuths

Installation of the 2nd generation SOVs commenced in late 2019 and finished in March 2020 (Figure 1), followed by an extensive series of tests aiming to optimise the performance. A detailed description of the testing sequence and the outcomes is provided in Correa (2021).

After initial testing, the following acquisition parameters were set for the vibrators:

- 1st generation: Large motors only, stationary to 80 Hz, 150 s quadratic sweep, i. e., instantaneous frequency is increasing as time squared.
- 2nd generation: Large motors performing the same length quadratic sweep covering frequencies up to 80 Hz while smaller motors operating with linear sweep 105-70 Hz.

2.4 Continuous monitoring using the DAS/SOV array

The CO_2 injection is monitored using only the engineered Constellation fibre deployed behind the well casings. These fibres are connected to three DAS interrogators:

- iDASv3#1 – CRC4 (first) & CRC3 (second)
- iDASv3#2 – CRC7 (first) & CRC6 (second)
- iDASv3#3 – CRC5 (first) & 1 km long helically would cable (HWC) buried between Pad C and Pad B at ~ 1 m depth.

The HWC cable was not directly used for the plume monitoring. It was installed and connected to evaluate the performance of the cable itself (Tertyshnikov et al., 2020).

With this setup, DAS data are acquired continuously and time-stamped using GPS timing units. The acquisition commenced on 22/04/2020 and is still ongoing (as of 05/05/2021) continuously, apart for few operational gaps. For the DAS units no. 1 and 2, these gaps do not exceed 3.5% of the overall duration of the survey. DAS no. 3 unit connected to CRC-5 failed September 11, 2020, and was replaced October 30, 2020, leaving a gap of more than a month. This happened before the start of the CO_2 injection and did not compromise the monitoring.

In parallel to DAS data acquisition, SOV sources have been operating in the production mode since early June 2020. SOV operation was suspended for two 4D VSP monitor survey acquisitions in 2021 and for several short gaps related to site or equipment maintenance activities.

A single vintage of DAS/SOV data is acquired over a period of 2 days, having each source operating for 2.5 hours, apart from SOV6, which operates for 5 hours. Each 2.5 hour period of operation consists of 44 sweeps with 150 s length, half clockwise and half counterclockwise, with a 5 s listen time between each rotation. SOVs are asynchronous and thus do not control the phase of rotation (Freifeld et al., 2016), and, as such, data processing requires GPS time-stamped recording of a reference geophone buried beneath the source. SOVs are operated during the daytime only to minimise disturbance to the farming community.

A single day of acquisition of DAS data from the five wells and the HWC cable produces about 1.6 TB of data. By the beginning of May 2021, over 0.5 PB of raw data had been acquired. These data volumes greatly exceed the capacity of conventional Internet connections available at the site. As such, data acquisition and processing were automated and performed on-site using a dedicated computing facility. This is done using an in-house-developed software package, which controls seismic sources, facilitates data transfers and performs the complete time-lapse VSP processing sequence. Processed data is uploaded to the cloud storage at different processing stages available for direct visual inspection and for more advanced processing performed at the Curtin office in Perth. The typical size of the daily data transfer is below 500 MB. A more detailed description of the DAS/SOV system used at the Otway site can be found in Isaenkov et al. (2021).

2.5 Acquisition of baseline and monitor 4D seismic surveys

The CO2CRC Otway Project Stage 3 seismic monitoring program is built upon the experience and findings of Stage 2C, and many components and parameters are inherited from the previous surveys acquired at the site. Stage 2C had six vintages of surface and borehole 3D seismic, the baseline (B) and five monitor surveys (M1-M5) (Popik et al., 2020). Baseline (B) and M1-M3 surveys have the same acquisition geometry. During M4 survey acquired in January 2017, the area covered by shot points was extended in the Western direction to improve the characterisation of the future CRC-3 well location. CRC-3 was drilled later in 2017 and provided an opportunity to acquire a 3D VSP survey with

cemented fibre-optic cables and two DAS interrogators, Silixa iDAS v2 and Fotech Helios Theta during M5 (the final Stage 2C survey acquired in February-March 2018) (Correa et al., 2018b). This survey forms one of the two available baselines for the Stage 3 4D VSP dataset. Thus, for all Stage 3 3D seismic surveys, it is convenient to continue the numbering convention established for Stage 2C (M5-M8). The shot-point map for this and the following seismic surveys is shown in Figure 3; the source parameters are presented in Table 2.

Table 2. Source parameters (same for all surveys)

Seismic source	INOVA UniVib, 26,000 lbs
Sweep type	Linear
Number of sweeps per point	1, 70% peak force
Sweep duration	24 s, 0.5 s taper at either end of the sweeps, cosine
Start/end frequencies	6-150 Hz

Note that the EBS1 Constellation fibre installed in CRC-3 fibre-optic was not used during the M5 survey as the corresponding iDASv3 interrogator was unavailable.

After drilling and instrumenting of the new wells, in March-April 2020, another baseline survey, M6, was acquired using the 5-well array and iDAS v3 interrogators connected to the engineered fibre, with the same configuration used for DAS/SOV operation (Table 3).

Table 3. Survey parameters

Survey	M5	M6	M7	M8
Date	Feb-18 - Mar-18	Mar-20 - Apr-20	Jan-21	Mar-21
Wells	CRC-3	CRC-3, CRC-4, CRC-5, CRC-6, CRC-7		
Type of fibre	Single-mode	Constellation		
DAS interrogator	iDAS v2, Fotech Helios Theta	3 x iDAS v3		
Source line spacing	~50-100 m	~100 m		
Source step	15 m			
Number of source positions	4738	4084	3085	4317

Survey area (source distribution, km^2)	7.3	7.3	5.4	7.3

The original plan for the M6 survey was to use a similar but slightly expanded shot point coverage as in M5. The survey was scheduled to start March 18, 2020, with the Curtin University crew mobilising to the site two days ahead, March 16. However, on that date, Victoria declared a state of emergency in relation to the COVID-19 pandemic (Storen and Corrigan, 2020). Thus, the original plans had to be urgently reviewed with various parts of the survey area given different priories. Previous studies done for the site using both the buried geophone array and 3D VSP DAS in CRC-3 (Correa, 2018; Popik et al., 2019) indicated that decreasing the source density by 50% while retaining the overall areal shot point coverage is likely to have an only mild impact on the image quality. Thus, the focus was on retaining the spatial coverage while reducing the density of the survey.

The original Curtin crew acquired only 3037 source points prior to forced departure from the site, just ahead of the introduction of Western Australia's restrictions on interstate arrivals (Storen and Corrigan, 2020). The initial assessment of the fold map indicated that more points needed to be acquired. To this end, a local resident with suitable experience in vibroseis operation was identified by the Curtin team, and a replacement crew was formed, which acquired an extra 1047 shot points ahead of rapidly deteriorating weather and ground conditions. In order to do this, all DAS equipment was reconfigured for continuous acquisition. Data frames containing sweeps were extracted using information from the seismic signature recorder attached to vibroseis electronics, including GPS time and coordinates of the shot-point locations. While no real-time quality control was possible, each day of the remote acquisition, the data were correlated on-site and checked manually from the Perth office. Overall, 4084 source points were acquired, e.g. ~86% of the M5 source count.

Due to frequent changes to COVID-related Australia's interstate travel restrictions in 2021, the two monitor surveys (M7 and M8) were also acquired using the same local crew with remote supervision and quality checks.

The first monitor survey (M7) was acquired in January 2021 after the injection of 4382 t of supercritical CO_2-rich fluid into the subsurface. As the plume was expected to be small and to reduce the duration of the survey, the source coverage was reduced by removing shot points corresponding to far offsets on both eastern and western flanks. However, as M5 could provide an extra baseline, especially for the small plume surrounding the CRC-3 well, M7 included some of the shot points omitted in M6.

The second monitor survey (M8) was acquired in late March 2021. All the M6 and M7 source positions and extra positions from M5 were repeated.

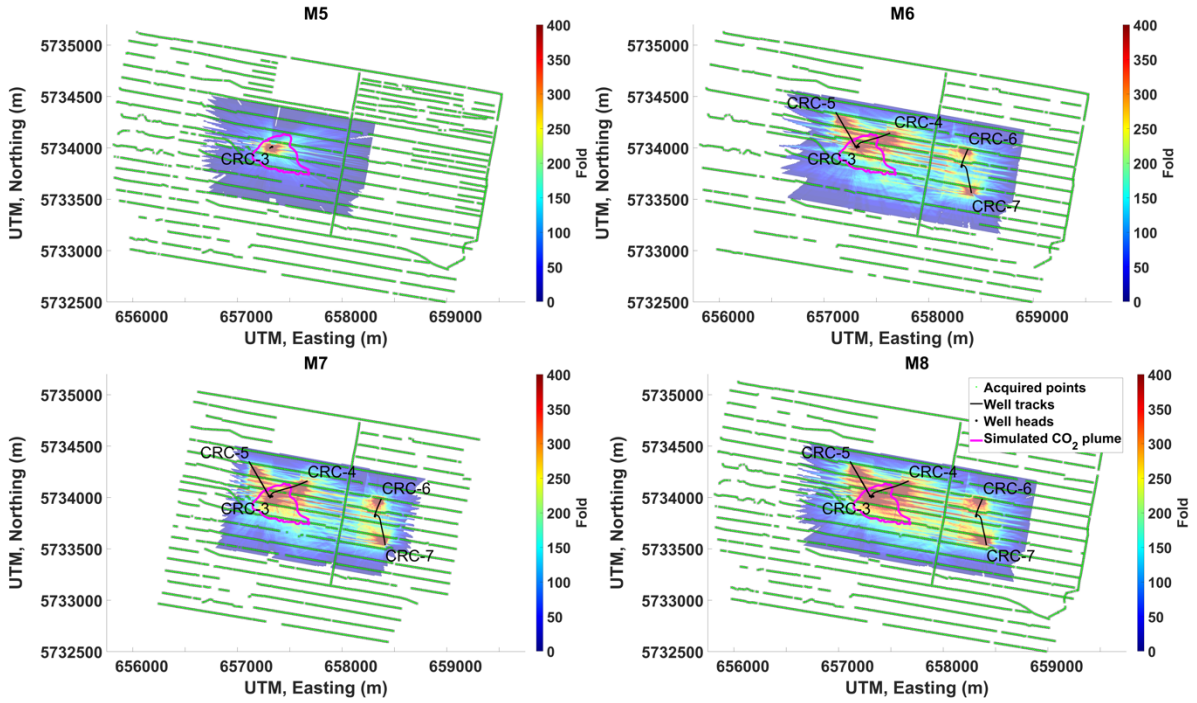

Figure 3. Lateral distribution of seismic shot points. Acquired shot points for each vintage are marked with green dots. Color-coded map shows seismic fold computed for receiver spacing of 5 m and 7.5x7.5 m bin size, combined for all wells. The pink contour shows the projection of the edge of the simulated plume at the end of the injection.

3 Results of initial data analysis

3.1 Continuous monitoring using SOVs

Figure 4 shows time delays in the arrival of the direct P wave on the DAS channels located at the bottom section of CRC-3, the CO_2 injector. This figure shows a sharp increase in time delays one day after the start of injection (1/12/2020); on the next day, we see a clear response on SOV9, which corresponds to the plume formed by approximately 90 t of CO_2. We see that the time-delay pattern is evolving during the injection, reflecting the evolution of the plume itself.

CRC-3 is perforated between 1536 and 1547 m MD, coinciding with the region where the time delay is noted to increase. For all SOVs, the maximum time delay reaches ~0.3-0.4 ms. For some of the SOVs, this time delay decreases gradually with increasing depth below the injection horizon (like SOV6 and SOV8). This decrease can be explained by the limited lateral extent of the plume. Its effect on the apparent direct-wave arrival time decreases with the increasing depth of receivers below the plume, which is attributed to wave diffraction around the plume boundary (Al Hosni et al., 2016).

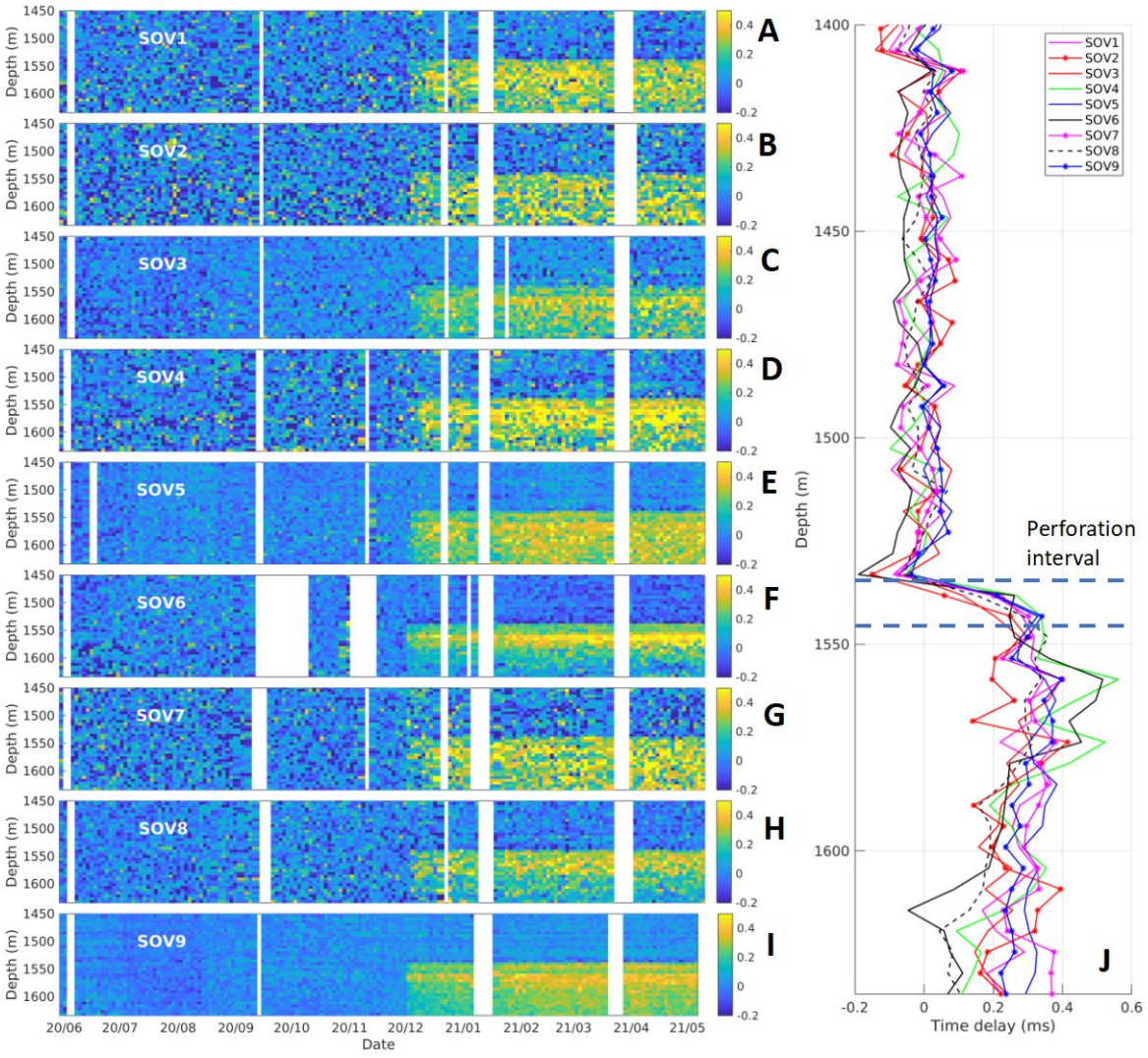

321 *Figure 4. Time delay analysis for CRC-3: time delays of the first break arrivals in the vicinity of the*
322 *injection interval versus time for SOV1-SOV9 (plots A-I) and average post-injection time delay curve*
323 *(plot J).*

324 The main source of information about the spatial distribution of the CO_2 is the set of 45 sections (all
325 possible combinations of 9 SOVs and 5 wells) obtained by seismic migration of the primary PP
326 reflections from the reservoir layer. The corresponding data processing flow was developed first in
327 commercial software (RadExPro) (Yavuz et al., 2020) and then implemented in Matlab as a stand-alone
328 software package for autonomous on-site processing (Isaenkov et al., 2021). This final processing flow
329 is summarised in Table 4.

330 *Table 4. DAS/SOV processing flow*

Procedure	Parameters
1. Data decimation	Output data has channel spacing of 5 m and time sampling of 2 ms
2. DAS data for individual sweeps extracted from the continuous record and deconvolved with the sweep recorded by the reference geophone installed next to SOV.	Deterministic deconvolution in Fourier domain, 0.1 white noise level
3. Vertical stacking	22 sweeps for each rotation direction
4. Geometry	Source and receiver geometry assigned
5. Deconvolution with an estimated wavelet and bandpass filtering	Fourier domain, individual for each rotation, wavelet estimated by averaging downgoing P waves
6. Stacking rotations	Data acquired from opposite rotation direction staked to form vertical source polarisation
7. Wavefield separation	F-K filtering to isolate target PP reflections, bottom muting past source-generated S-wave arrival
8. Amplitude correction	Compensation for the spherical divergence
9. Migration	Kirchhoff migration: central dip = 0, dip range = 7 degrees, 1D isotropic velocity function from VSP in the CRC-3 well

331

332 We illustrate the processing and imaging using the SOV6/CRC4 pair as the image obtained from this
333 pair represents the vertical plane passing through the injector well. An example of data obtained after
334 the deconvolution using the wavelet (step 5 from the table above) is shown in Figure 5. The time-lapse
335 response after injection of three different CO_2 volumes is shown with an orange arrow.

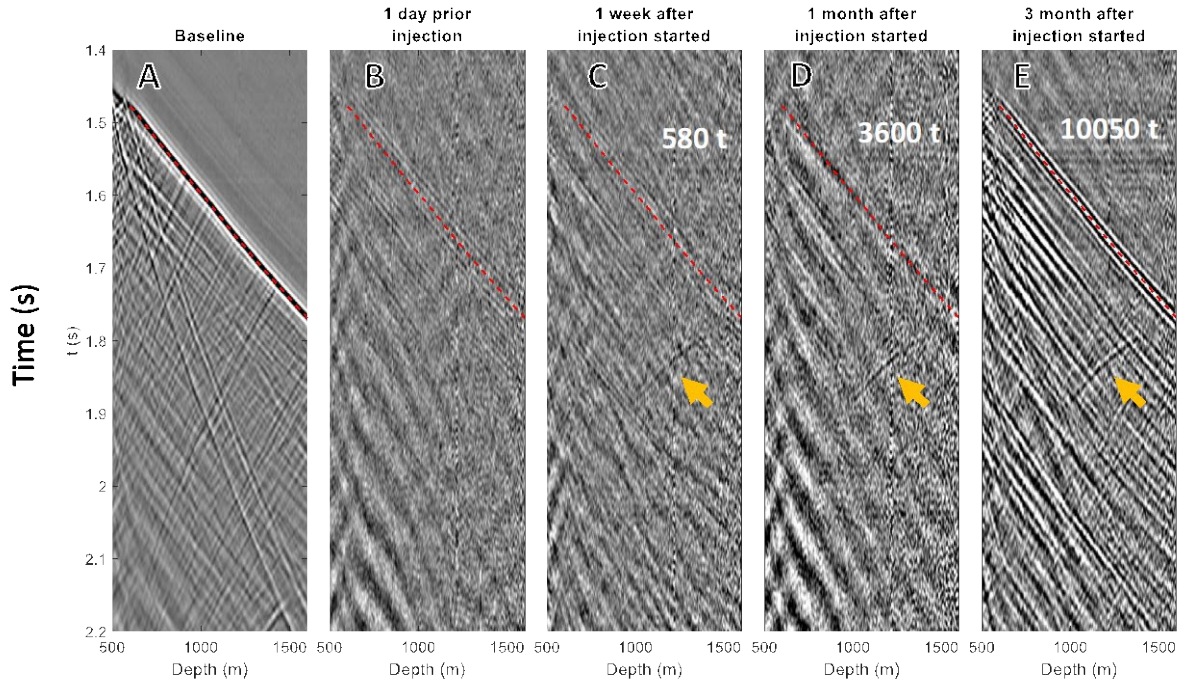

337 *Figure 5. Baseline (A) and difference (B-E) seismograms for SOV6/CRC4 pair after signature*
338 *deconvolution. Gain on the difference seismograms is increased by a factor of 10 as compared to the*
339 *baseline. Monitor seismograms B, C, D and E, correspond to 0 t, 580 t, 3600 t and 10000 t of the injected*
340 *CO_2, respectively.*

341 The difference seismograms (Figure 5C-D) show a clear plume signal after injection of the first few
342 hundreds of tonnes and its evolution with time. The baseline for the difference seismograms was
343 produced by stacking ten vintages (~20 days) of data just before the injection.

344 Notably, the level of time-lapse noise is increasing with the time interval between the baseline and
345 monitor, with surface-generated downgoing multiples exhibiting a low degree of repeatability. For
346 offset VSP geometry (as opposed to the zero-offset case) travel time curves for the direct P-wave and
347 those multiples are not, in general, parallel. As such second pass of deconvolution, which uses wavelet
348 averaged along the first breaks, cannot completely compensate for temporal changes in the near-
349 surface.

350 Figure 6 shows the final migrated image for SOV6/CRC4 pair, difference seismograms and NRMS
351 sections. NRMS values (away from the time-lapse target reflection) computed in 40 m vertical window,

in general, correspond below 20% for the monitor surveys within a month from the baseline and increase slightly to ~30% thereafter.

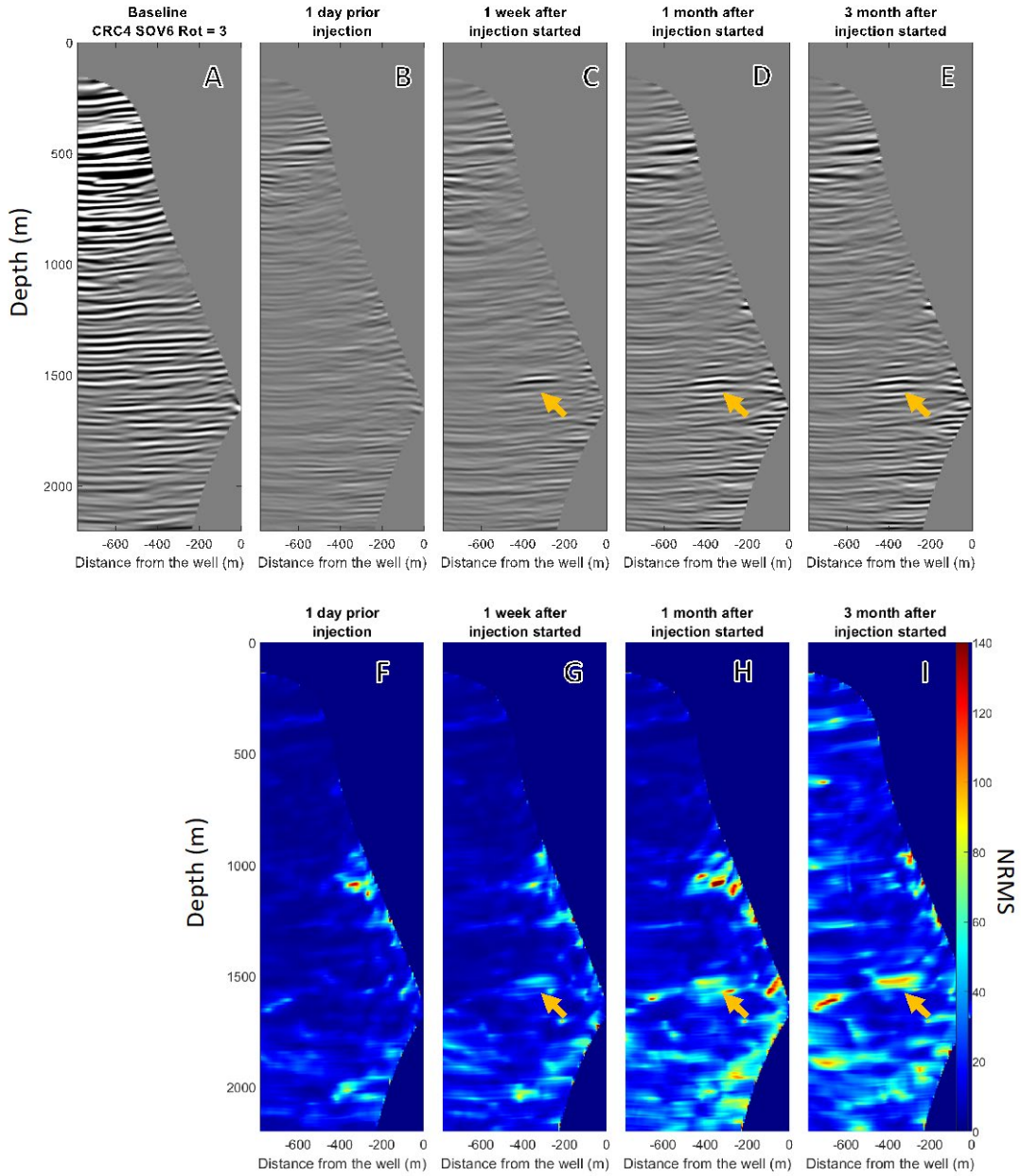

Figure 6. Baseline (A), difference seismograms (B-E) and NRMS sections (F-I) for SOV6-CRC4 pair after migration. Gain on the difference seismograms is increased by a factor of 3 as compared to the baseline. Monitor seismograms B, C, D and E and NRMS sections (F-I) correspond to 0 t, 580 t, 3600 t and 10000 t of the injected CO_2, respectively.

359 The orange arrows in Figure 6 shows the location of the gas-related anomaly. The anomaly is growing
360 in size, indicating the evolution of the plume on an individual SOV/well transect. Joint analysis of 4D
361 VSP and continuous monitoring is discussed in the next section.

362 3.2 Fast track processing of multi-well 4D VSP data

363 For the fast-track processing of the 4D VSP data, we perform 'parallel' processing of the individual
364 datasets with cross-equalised acquisition geometry using the same processing flow for each vintage.
365 Moreover, at this stage, we process 3D volumes for each well separately and do not merge images
366 together. The processing flow, developed initially for baseline data, is detailed in Yurikov et al. (2020)
367 and summarised in Table 5.

368 *Table 5. 3D VSP processing flow*

Procedure	Parameters
3D geometry assignment	Source and receiver geometry assigned
Vertical stacking of adjacent traces	5 m
Correlation	Correlation with the source sweep
First break picking	Semi-automated
Wavelet extraction and deconvolution	Impulse width = 300 ms
2D spatial filter	Number of samples: 1; number of traces: all
Bandpass filters	Ormsby 0-20-80-160 Hz, 5-10-90-180 Hz
Wavefield separation	F-K filter attenuating down-going waves; F-K filter attenuating up-going PS and S waves
Amplitude correction	Time raised to power of 2;
Bottom mute	Muted below direct S-wave arrival
Resample	2 ms
3D migration	Kirchhoff migration: central dip = 0, dip range = 7 degrees, 1D isotropic velocity function from VSP in the CRC-3 well

369

370 Figure 7 shows a vertical section from the 3D baseline and difference volumes for the two monitor
371 surveys for the CRC-3 and CRC-4 wells. The time-lapse signal from the CO_2 injection is marked with an
372 orange arrow. The difference between the lateral amplitude distribution on reflectors for different
373 wells are related to differences in illumination/directivity.

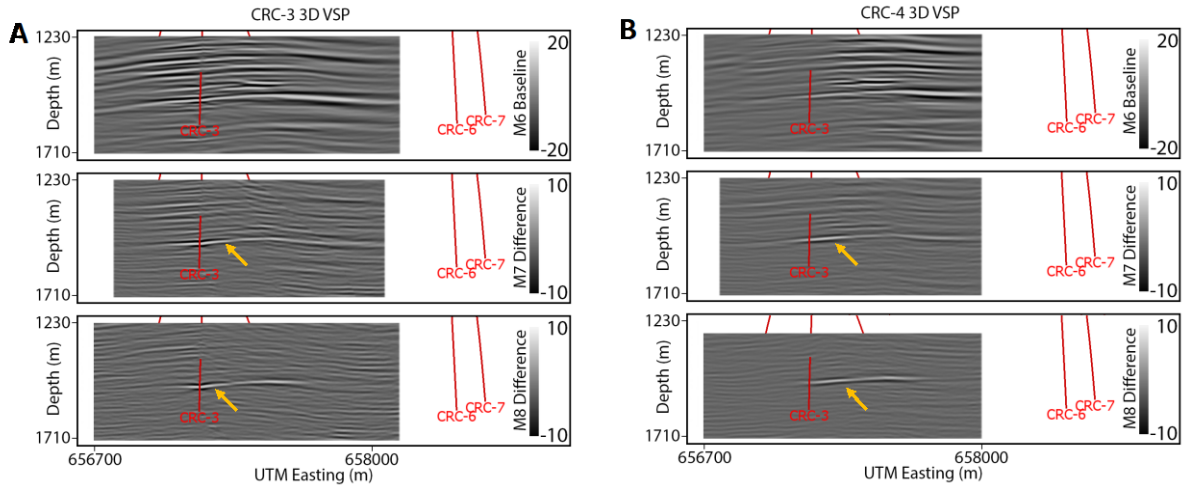

375 *Figure 7. Results of fast track processing of 4D VSP data for CRC-3 (A) and CRC-4 (B) wells: vertical slice*
376 *through the injector well in the west-east direction.*

377 The lateral extent of the time-lapse anomalies for M7 and M8 3D VSP surveys is shown in Figure 8
378 using energy attributes computed at the target horizon from the CRC-3-7 data. Time-lapse anomalies
379 look consistent across the different wells except for CRC-5, where the quality of the image deteriorates
380 in the south-eastern quadrant due to a significantly lower fold in that area. CRC-5 is also the only well
381 where the interrogator was replaced between M6 and M7/M8 surveys due to a hardware fault.

382 Yellow contours in Figure 8 show the extent of the plume interpreted from SOV data corresponding
383 to the start of the acquisition of each monitor 3D survey, M7 and M8. In order to obtain these
384 contours, all SOV/Well transects corresponding to the two vintages were loaded together with 3D VSP
385 volumes, and the extent of the anomaly was manually picked on each transect. Figure 9 shows a
386 comparison between 4D VSP (CRC-4) and time-lapse offset VSP (SOV9/CRC-3) difference seismograms.

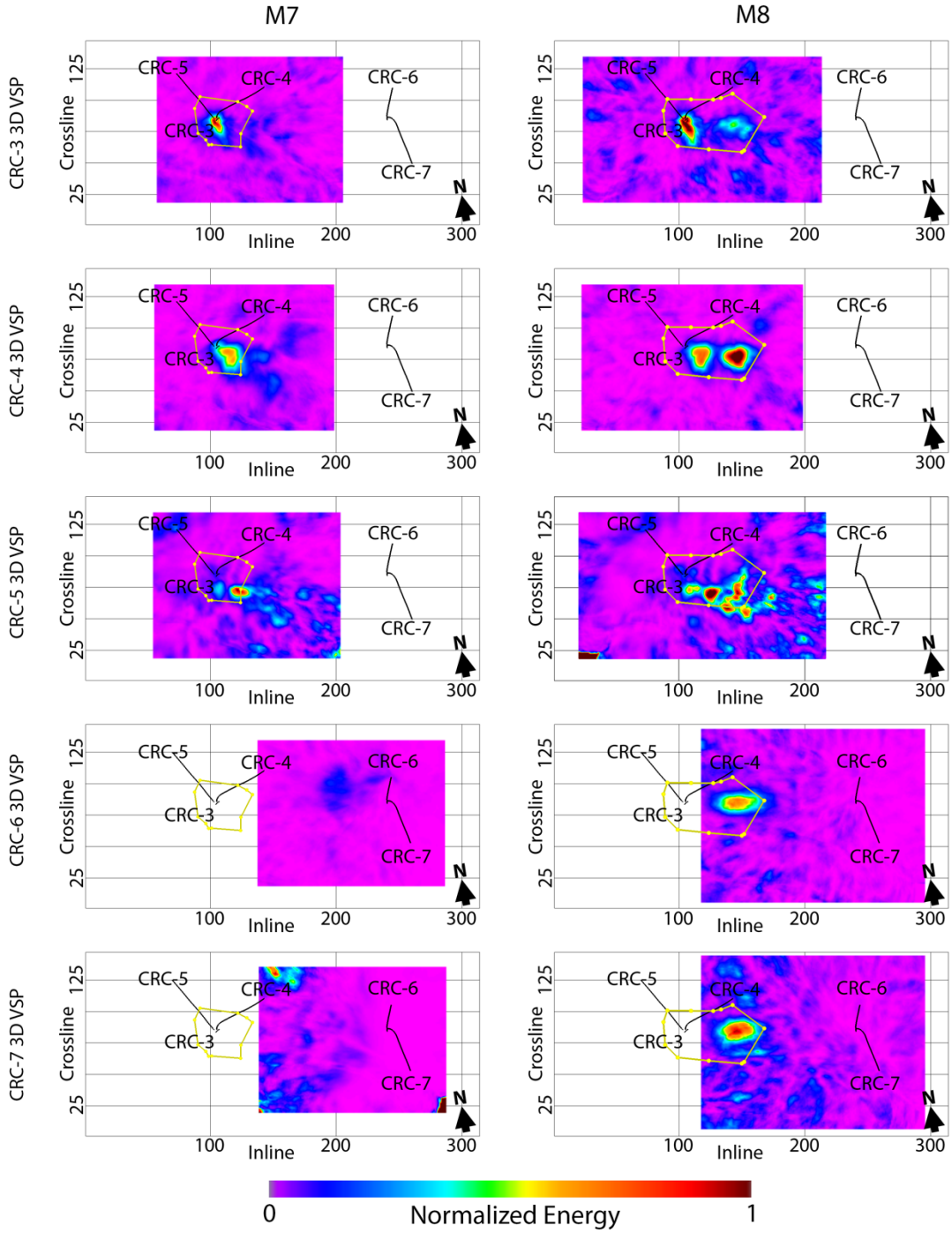

388 *Figure 8. The energy of time-lapse difference (30 m vertical window) for CRC-3-6 wells from 4D VSP.*

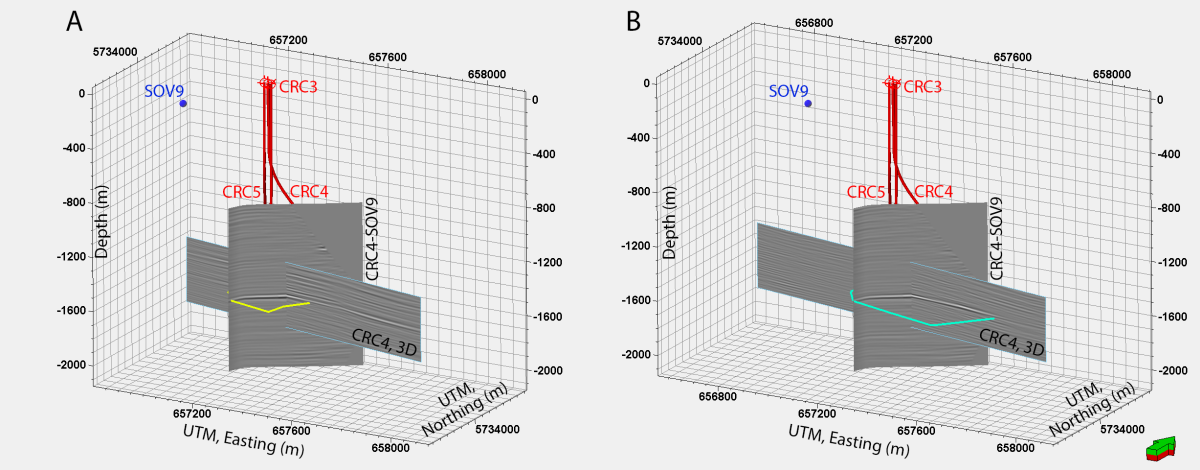

Figure 9. Comparison of migrated difference sections of 4D VSP (CRC-4) for M7 (A) and M8 (B) surveys juxtaposed with the corresponding SOV (CRC4/SOV9) sections. Yellow (A) and teal (B) contours correspond to the plume extend interpreted from SOV data acquired just before 3D VSP acquisition commenced.

4 Discussion

4.1 Surface vs Borehole geometry

Analysis of the initial results suggests that time-lapse seismic in borehole configuration is a powerful tool for CO_2 plume imaging. Several projects also reported successful deployment of downhole seismic to monitor small-scale CO_2 injections (Daley et al., 2008; Tertyshnikov et al., 2019b). The key advantages of downhole methods which contributed to this are as follows:

The principal benefit of VSP geometry for seismic monitoring is a much smaller degree of disturbance to other land users, such as farmers. This is common for any permanent receiver installation (with borehole playing the role of 'permanent installation' even if conventional VSP tool is used through intervention).

Much lower noise level than surface seismic, and the high repeatability of the acquisition geometry results in a greater level of data repeatability. Thus, the borehole seismic setup detects smaller signals, which is important for the early detection of CO_2 leaks and in detecting the leading edge of a plume.

Borehole seismic allows the use of both down-going and up-going waves. The direct P wave gives a good estimate of the far-field source signature (Poletto et al., 2016) and is widely used to perform deconvolution in VSP data processing. This is useful for cross-equalisation of the different vintages in time-lapse seismic and improving the resolution of the data.

There are added benefits of placing seismic receivers all the way to, or even below, the injection interval. Proximity to the injection interval eliminates blind spots in illumination, which, for instance, has affected 4D VSP at Aquistore (Harris et al., 2017). By monitoring reflectivity changes above the storage interval as well as travel time delays within and below the injection interval can help to constrain velocity-saturation relations (Al Hosni et al., 2016).

All of the benefits listed above helped detect the time-lapse signal from the CO_2 plume beginning the first day after the start of injection as detected by SOV 9 (Figure 4). Within the first week, the plume was spatially delineated along multiple well-SOV pairs (Figure 5 and 6).

A conventional surface seismic survey, particularly with a dense array of source and receiver points covering a large areal region, provides imaging capabilities that cannot be matched with a VSP acquisition. The drawback, of course, is that survey cost and land impacts scale with survey size. While 4D VSP cannot replicate surface seismic spatial coverage, it provides a cost-effective approach that meets specific containment and conformance requirements associated with CO_2 sequestration (Bacci et al., 2017). Notable benefit of VSP for CO_2 sequestration monitoring is that the activity is synergistic with other monitoring requirements, such as pressure and geochemical monitoring, which require offset monitoring wells. VSP acquisition, with its focus at the well, also has a very low threshold of detection for above zone leakage that can arise from a well integrity issue.

In the Otway Stage 3 experiment, the useful image extends to ~800-900 m from each of the boreholes, e.g., roughly half of their depth. Extending the range further can, in principle, be achieved by employing seismic interferometry (Schuster, 2009) using surface-generated multiple reflections. Initial

tests performed for the Otway site (Sidenko et al., 2019) confirm the feasibility of this approach, but more research is still required.

4.2 3D VSP vs offset VSP geometry

While at this stage, 4D VSP cannot replace surface seismic when large spatial coverage is required, for small-scale experiments, like Stage 3, it is sufficient for imaging the plume.

One of the issues we see from the initial 4D VSP data analysis is that the plume shape while remaining broadly consistent, varies from well to well. This was to be expected as the illumination for each well is different. The plume, in our case, is a spatially small object, less than a few hundred meters in diameter, so changes in illumination and imperfection of the 1D velocity model play a significant role in the final image. Additionally, the Otway area is known to have significant vertical and azimuthal seismic anisotropy (Popik et al., 2021), which was not yet taken into account in the imaging. The ability to focus the image of a small 4D object using multiple wells can be used as a tool to QC the velocity model.

Offset VSP geometry refers to the scenario where a single source position or a small number of those used to acquire the data. In many cases, offset VSP is treated as a cost-efficient method, which can provide an image of the subsurface along a semi-vertical surface. Moreover, offset VSP geometry has certain advantages over 4D VSP (and surface 4D seismic). The acquisition of an individual survey is very quick, especially if it is done with wells instrumented with DAS. This gives an opportunity to monitor rapid processes, such as the evolution of a very small plume or above zone leakage. In Stage 3, we used this advantage by employing permanent sources, the SOVs, but conventional seismic sources can also be used (Tertyshnikov et al., 2019a).

In principle, data processing flows for 4D VSP and continuous monitoring using SOVs were designed in a similar fashion in order to allow for direct comparison between the images. However, the plume image obtained from offset VSP geometry looks slightly larger (Figure 8) due to an attempt to image

small 3D object using only (pseudo) 2D geometry, so that reflection points located within the plume but outside of the imaging plane still contribute to the image.

4.3 Vibroseis vs SOV

The reduced frequency content of SOVs, 8 Hz-105 Hz as compared to 6 Hz-150 Hz for vibroseis contributes to lower spatial resolution. Figure 10 shows the comparison between deconvolved data for SOV and the nearest shot point acquired with vibroseis. SOV data has two rounds of deconvolution applied, all the sweeps in one sweep set and both rotation directions stacked (this corresponds to step 6, Table 4). The difference between frequency bands for the sources is significantly pronounced for the small offsets (Figure 10, A). For the larger offsets (Figure 10, B), the difference in the frequency contents for both conventional vibroseis and SOV data decreases as high frequencies are affected by seismic attenuation. Note that the signal-to-noise ratio (ratio of RMS amplitudes computed in 100 ms window around the first break and the same length window before the first arrivals) for the SOV data is at least 2-4 times higher than the one for vibroseis. This is because the SOV seismogram is using ~2.5 hours of stacked sweeps as opposite to a single 24 s sweep for the vibroseis.

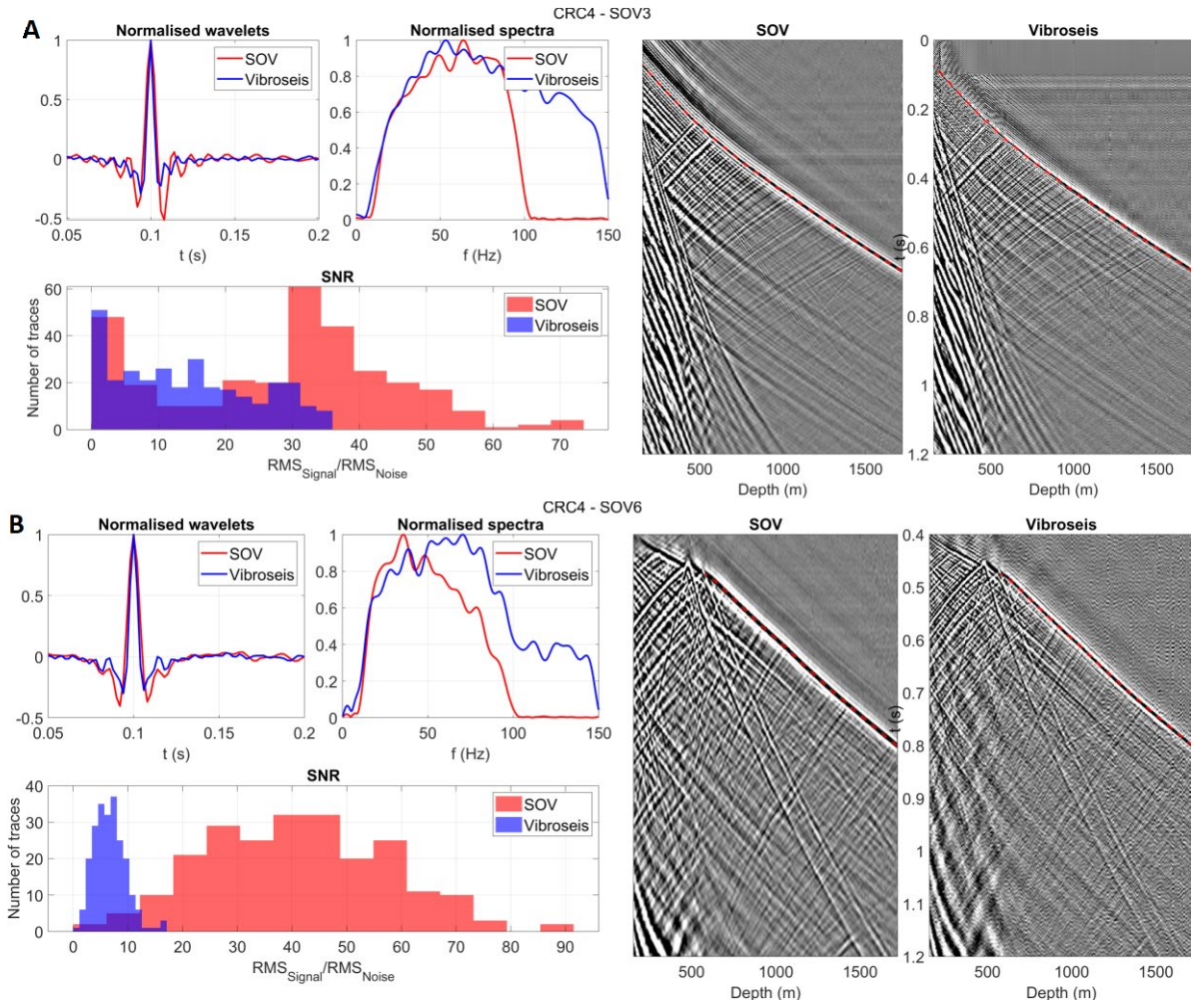

471 *Figure 10. Source wavelets, their amplitude spectra, signal-noise ratios and seismograms for vibroseis*
472 *and SOV for near (A, CRC-4, SOV3) and far (B, CRC-4, SOV6) offsets.*

473 The big advantage of a permanent remotely operated seismic source, like SOV, is the ability to acquire
474 the data without having a seismic crew on site. Most of the time, the SOV source equipment operated
475 autonomously, with very little maintenance effort required from the technical personnel on-site.
476 However, there was a couple of failures where some equipment had to be replaced. The simplicity of
477 the SOV design, where most of the components are commercially available off-the-shelf products
478 used by multiple industries, gave an opportunity to promptly conduct the repairs, even when logistics
479 was heavily affected by the pandemic.

4.4 DAS vs geophones

The main Stage 3 data are acquired using DAS with the benefit of an engineered fibre that increased signal beyond that of a standard telecommunications single-mode fibre. Advantages of using fibre-optic cables cemented behind the casing include very low noise, the longevity of the installation and leaving all the in-well space free for other equipment. Such installations allow the data acquisition from the entire length of several wells with a single source excitation.

An obvious problem with this approach is that the cable needs to be installed at the time of drilling, limiting the ability to retrofit existing wells. However, fibre-optic cables can be attached to production tubing or allowed to be freely hanging with only modest penalties in sensitivity. For instance, the tubing-conveyed cable in CRC-2 was used during Stage 2 (Correa et al., 2019). A direct comparison between the various methods of deploying fibre performed using the newly drilled wells demonstrated that the decrease in sensitivity due to weaker coupling is relatively small (Pevzner et al., 2020b).

DAS measures only a single component of strain (rate), as opposed to 3C geophones, which provide three components of particle velocity. This fact complicates deriving the source wavelet for deconvolution using traces corresponding to high angles of incidence / relatively shallow depths of the well. For the Stage 3 configuration, the maximum offsets from downhole receivers to seismic sources reaches ~2 km. The directionality of DAS supports installing optical fibre to the bottom of a deep well, where angles between the direct P wave rays and the well are still relatively small. The deeper traces (excluding the section below the injection level in CRC-3) will provide the highest signal quality and the best data for deriving the source wavelet.

The Otway site has a number of different fibres installed in the cemented cables, including single-mode and two different engineered fibres. This gives an opportunity to compare the performance between fibres. To date, the project data have been acquired using single-mode (M5, various tests) and Constellation fibre (M6-M9). In principle, just having a conventional single-mode fibre may be

sufficient to image the plume. A previous study at Otway showed that using the enhanced-backscattering increases DAS sensitivity by about 14 dB (~5 times) (Correa et al., 2017). This difference has an important implication on the source effort requirements. The same area can be imaged by using different source densities and/or different numbers of repeated source excitations for each source point. Increasing the number source position or the number of excitations leads to a higher signal to noise ratio, higher duration and cost of the survey. To achieve the same noise floor (assuming purely random white noise), the standard fibre requires an increase of the overall source effort by a factor of 25. This fibre is paired with the equipment from a specific vendor. Having enough spare fibres, including generic single- and multi-mode ones, in the sensing cable is important to de-risk the dependence on the specific equipment availability and future-proof the installation.

5 Conclusions

Seismic monitoring in the Stage 3 of the Otway project employs two different VSP acquisition geometries, 3D VSP using conventional vibroseis trucks and offset VSP with SOVs. The role of 3D VSP, which is a more conventional technique, was to provide a benchmark for continuous offset-VSP monitoring with permanent sources.

The main phase of the experiment was concluded by May 1, 2021, with baseline and monitor data successfully acquired for both modalities. While in-depth data analysis requires further work, the currently available results allow us to make some interim conclusions.

The CO_2 injection was successfully detected by both seismic techniques. 4D VSP data provided the image of the plume for the two monitor surveys acquired at ~4 and ~12 kt of injection. Continuous monitoring using SOVs was able to track the plume evolution from the first days of injection.

While the plume image is broadly consistent between data obtained from different wells and different techniques, there are some differences. On the one hand, more work is required to fully understand

the causes of these differences. On the other hand, these differences give an excellent opportunity to understand the uncertainty of a time-lapse image.

Continuous seismic acquisition with a multi-well DAS installation generates data volumes that far exceed the bandwidth of currently available options for data transfer using the Internet. This has prompted the deployment of automated on-site processing, using dedicated purpose-built software, which is run on computing facilities deployed at Otway. Automated on-site processing eliminates delays between data acquisition and availability of processing results, thus fixing one of the pitfalls of seismic monitoring applications. In addition, having the main site recording systems designed to be operated remotely was a key factor that enabled smooth running of the experiment during the global pandemic, when travel to the site was heavily restricted most of the time.

Robustness and simplicity of the permanent seismic sources, the SOVs, allowed continuous data acquisition for over a year, with maintenance performed by local technical personnel available at the site.

Continuous monitoring commenced seven months prior to injection, which provided baseline DAS/SOV data that covers both wet and dry seasons and gives detailed information on the variations of the repeatability over time. This forms the basis for an in-depth analysis of the monitor data, which also covers the transition from dry to wet surface conditions. An extended baseline is also important for the analysis of injection-induced seismicity, where it can provide information about the presence and distribution of the natural seismicity in the area and allow for discrimination between the natural and induced seismicity when the injection will commence.

The initial seven months prior to injection were also helpful for rectifying equipment malfunctions and the development of response procedures. As a result, the most critical part of the experiment, monitoring the actual CO_2 injection, proceeded virtually faultless.

Finally, having multiple cables, a variety of fibres, and permanently deployed seismic sources, which can be operated remotely, makes the Otway site one of the most advanced in-situ research facilities for fibre-optic sensing and seismic imaging and monitoring.

6 Acknowledgements

The Otway Project received CO2CRC Ltd funding through its industry members and research partners, the Australian Government under the CCS Flagships Programme, the Victorian State Government and the Global CCS Institute. The authors wish to acknowledge the financial assistance provided through Australian National Low Emissions Coal Research and Development (ANLEC R&D). ANLEC R&D is supported by COAL21 Ltd and the Australian Government through the Clean Energy Initiative. Funding for LBNL was provided through the Carbon Storage Program, U.S. DOE, Assistant Secretary for Fossil Energy, Office of Clean Coal and Carbon Management through the NETL, under contract No. DE-AC02-05CH11231. The authors thank Michael Mondanos and Stoyan Nikolov (Silixa inc.) for help with the fibre-optic equipment and Peter Dumesny (Upstream Production Solutions) for invaluable help with all aspects of field operations.

7 References

Ajayi, T., Gomes, J.S., Bera, A., 2019. A review of CO2 storage in geological formations emphasizing modeling, monitoring and capacity estimation approaches. Petroleum Science 16, 1028-1063.

Al Hosni, M., Caspari, E., Pevzner, R., Daley, T.M., Gurevich, B., 2016. Case History: Using time-lapse vertical seismic profiling data to constrain velocity–saturation relations: the Frio brine pilot CO2 injection. Geophys Prospect 64, 987-1000.

Andersen, J.K., 2019. Automated High Power Permanent Borehole Seismic Source Systems for Long-Term Monitoring of Subsurface CO2 Containment and Storage. ; GPUSA Inc., p. Medium: ED.

573 Arts, R.J., Zhang, X., Verdel, A.R., Santonico, D., Meekes, J.A.C., Noorlandt, R.P., Paap, B.F.,
574 Vandeweijer, V.P., 2013. Experiences with a Permanently Installed Seismic Monitoring Array at the
575 CO2 Storage Site at Ketzin (Germany). - A Status Overview. Energy Procedia 37, 4015-4023.

576 Bacci, V.O., O'Brien, S., Frank, J., Anderson, M., 2017. Using a Walk-away DAS Time-lapse VSP for CO2
577 Plume Monitoring at the Quest CCS Project. . Recorder 42, 18-21.

578 Barajas-Olalde, C., Adams, D.C., Kovacevich, J.T., Jin, L., Livers, A.J., Hamling, J.A., Gorecki, C.D.,
579 Cercone, D.P., Freifeld, B.M., 2020. CO₂ injection seismic monitoring without creating a
580 migrated image, SEG Technical Program Expanded Abstracts 2020, pp. 71-75.

581 Bauer, R.A., Will, R., E. Greenberg, S., Whittaker, S.G., 2019. Illinois Basin–Decatur Project, in: Wilson,
582 M., Landrø, M., Davis, T.L. (Eds.), Geophysics and Geosequestration. Cambridge University Press,
583 Cambridge, pp. 339-370.

584 Burnison, S.A., Livers, A.J., Hamling, J.A., Salako, O., Gorecki, C.D., 2017. Design and Implementation
585 of a Scalable, Automated, Semi-permanent Seismic Array for Detecting CO2 Extent During Geologic
586 CO2 Injection. Energy Procedia 114, 3879-3888.

587 Correa, J., 2018. Distributed Acoustic Sensing for Seismic Imaging and Reservoir Monitoring Applied
588 to CO2 Geosequestration, Exploration Geophysics. Curtin, Perth, p. 188.

589 Correa, J., Egorov, A., Tertyshnikov, K., Bona, A., Pevzner, R., Dean, T., Freifeld, B., Marshall, S., 2017.
590 Analysis of signal to noise and directivity characteristics of DAS VSP at near and far offsets — A CO2CRC
591 Otway Project data example. The Leading Edge 36, 994a991-994a997.

592 Correa, J., Freifeld, B., Pevzner, R., Wood, T., Tertyshnikov, K., Bona, A., 2018a. Continuous DAS VSP
593 monitoring using surface orbital vibrators: field trials for optimal configuration at the CO2CRC Otway
594 Project, 80th EAGE Conference and Exhibition 2018. EAGE, Copenhagen, Denmark, p. WS08.

595 Correa, J., Pevzner, R., Bona, A., Tertyshnikov, K., Freifeld, B., Robertson, M., Daley, T., 2019. 3D
596 vertical seismic profile acquired with distributed acoustic sensing on tubing installation: A case study
597 from the CO2CRC Otway Project. Interpretation 7, SA11-SA19.

598 Correa, J., Pevzner, R., Popik, S., Tertyshnikov, K., Bona, A., Freifeld, B., 2018b. Application of 3D VSP
599 acquired with DAS and 3C geophones for site characterization and monitoring program design:
600 preliminary results from Stage 3 of the CO2CRC Otway project, SEG Technical Program Expanded
601 Abstracts 2018, pp. 4933-4937.

602 Couëslan, M.L., Ali, S., Campbell, A., Nutt, W.L., Leaney, W.S., Finley, R.J., Greenberg, S.E., 2013.
603 Monitoring CO2 injection for carbon capture and storage using time-lapse 3D VSPs. The Leading Edge
604 32, 1268-1276.

605 Daley, T., Freifeld, B., Ajo-Franklin, J., Dou, S., Pevzner, R., Shulakova, V., Kashikar, S., Miller, D., Goetz,
606 J., Henninges, J., Lueth, S., 2013. Field testing of fiber-optic distributed acoustic sensing (DAS) for
607 subsurface seismic monitoring. The Leading Edge 32, 699-706.

608 Daley, T.M., Myer, L.R., Peterson, J.E., Majer, E.L., Hoversten, G.M., 2008. Time-lapse crosswell seismic
609 and VSP monitoring of injected CO2 in a brine aquifer. Environmental Geology 54, 1657-1665.

610 Freifeld, B.M., Pevzner, R., Dou, S., Daley, T., Robertson, M., Tertyshnikov, K., Wood, T., Ajo-Franklin,
611 J., Urosevic, M., Gurevich, B., 2016. The CO2CRC Otway Project deployment of a Distributed Acoustic
612 Sensing Network Coupled with Permanent Rotary Sources, 78th EAGE Conference & Exhibition 2016.
613 EAGE, Vienna, Austria, p. Tu LHR2 06.

614 Gurevich, B., Pevzner, R., Urosevic, M., Kepic, A., Shulakova, V., Caspari, E., 2014. 2D and 3D seismic
615 investigations for Stage 1 and 2C, in: Cook, P.J. (Ed.), Geologically storing carbon: Learning from the
616 Otway Project Experience. CSIRO Publishing, Australia, pp. 155-196.

617 Harris, K., White, D., Samson, C., 2017. Imaging the Aquistore reservoir after 36 kilotonnes of CO2
618 injection using distributed acoustic sensing. Geophysics 82, M81-M96.

619 Hartog, A.H., 2017. An Introduction to Distributed Optical Fibre Sensors. CRC Press.

620 Ikeda, T., Tsuji, T., Takanashi, M., Kurosawa, I., Nakatsukasa, M., Kato, A., Worth, K., White, D., Roberts,
621 B., 2017. Temporal variation of the shallow subsurface at the Aquistore CO2 storage site associated

622 with environmental influences using a continuous and controlled seismic source. Journal of
623 Geophysical Research: Solid Earth 122, 2859-2872.

624 Isaenkov, R., Pevzner, R., Glubokovskikh, S., Yavuz, S., Yurikov, A., Tertyshnikov, K., Gurevich, B.,
625 Correa, J., Wood, T., Freifeld, B., Mondanos, M., Nikolov, S., Barraclough, P., 2021. An automated
626 system for continuous monitoring of CO2 geosequestration using multi-well offset VSP with
627 permanent seismic sources and receivers: Stage 3 of the CO2CRC Otway Project. International Journal
628 of Greenhouse Gas Control 108, 103317.

629 Jenkins, C., Marshall, S., Dance, T., Ennis-King, J., Glubokovskikh, S., Gurevich, B., La Force, T., Paterson,
630 L., Pevzner, R., Tenthorey, E., Watson, M., 2017. Validating Subsurface Monitoring as an Alternative
631 Option to Surface M&V - The CO2CRC's Otway Stage 3 Injection. Energy Procedia 114, 3374-3384.

632 Jervis, M., Bakulin, A., Smith, R., 2018. Making time-lapse seismic work in a complex desert
633 environment for CO2 EOR monitoring — Design and acquisition. The Leading Edge 37, 598-606.

634 Johnston, D.H., 2013. Practical Applications of Time-lapse Seismic Data. SEG Books.

635 Lumley, D., 2010. 4D seismic monitoring of CO2 sequestration. The Leading Edge 29, 150-155.

636 Majer, E.L., Daley, T.M., Korneev, V., Cox, D., Peterson, J.E., Queen, J.H., 2006. Cost-effective imaging
637 of CO2 injection with borehole seismic methods. The Leading Edge 25, 1290-1302.

638 Mateeva, A., Lopez, J., Chalenski, D., Tatanova, M., Zwartjes, P., Yang, Z., Bakku, S., de Vos, K., Potters,
639 H., 2017. 4D DAS VSP as a tool for frequent seismic monitoring in deep water. The Leading Edge 36,
640 995-1000.

641 Mathieson, A., Midgely, J., Wright, I., Saoula, N., Ringrose, P., 2011. In Salah CO2 Storage JIP: CO2
642 sequestration monitoring and verification technologies applied at Krechba, Algeria. Energy Procedia
643 4, 3596-3603.

644 Mathieson, A., Midgley, J., Dodds, K., Wright, I., Ringrose, P., Saoul, N., 2010. CO2 sequestration
645 monitoring and verification technologies applied at Krechba, Algeria. The Leading Edge 29, 216-222.

Michael, K., Avijegon, A., Ricard, L., Myers, M., Tertyshnikov, K., Pevzner, R., Strand, J., Hortle, A., Stalker, L., Pervukhina, M., Harris, B., Feitz, A., Pejcic, B., Larcher, A., Rachakonda, P., Freifeld, B., Woitt, M., Langhi, L., Dance, T., Myers, J., Roberts, J., Saygin, E., White, C., Seyyedi, M., 2020. A controlled CO2 release experiment in a fault zone at the In-Situ Laboratory in Western Australia. International Journal of Greenhouse Gas Control 99, 103100.

Nakatsukasa, M., Kurosawa, I., Kato, A., Takanashi, M., White, D.J., Worth, K., 2016. The Performance of an ACROSS Permanent Seismic Source for Time Lapse Seismic at the Aquistore CO2 Storage Site, International Petroleum Technology Conference.

Pevzner, R., Tertyshnikov, K., Sidenko, E., Ricard, L., 2020a. Monitoring Drilling and Completion Operations Using Distributed Acoustic Sensing: CO2CRC Stage 3 Project Case Study, First EAGE Workshop on Fibre Optic Sensing. EAGE, Amsterdam, p. WeFOS09.

Pevzner, R., Tertyshnikov, K., Sidenko, E., Yavuz, S., 2020b. Effects of Cable Deployment Method on DAS VSP Data Quality: Study at CO2CRC Otway in-situ Laboratory, 82nd EAGE Annual Conference & Exhibition, Amsterdam, p. We_Dome3_11.

Pevzner, R., Urosevic, M., Tertyshnikov, K., AlNasser, H., Caspari, E., Correa, J., Daley, T., Dance, T., Freifeld, B., Glubokovskikh, S., Greenwood, A., Kepic, A., Popik, D., Popik, S., Raab, M., Robertson, M., Shulakova, V., Singh, R., Watson, M., Yavuz, S., Ziramov, S., Gurevich, B., 2020c. Chapter 6.1 - Active surface and borehole seismic monitoring of a small supercritical CO2 injection into the subsurface: experience from the CO2CRC Otway Project, in: Kasahara, J., Zhdanov, M.S., Mikada, H. (Eds.), Active Geophysical Monitoring (Second Edition). Elsevier, pp. 497-522.

Poletto, F., Schleifer, A., Zgauc, F., Meneghini, F., Petronio, L., 2016. Acquisition and deconvolution of seismic signals by different methods to perform direct ground-force measurements. J Appl Geophys 135, 191-203.

669 Popik, S., Pevzner, R., Bona, A., Tertyshnikov, K., Glubokovskikh, S., Gurevich, B., 2021. Estimation of
670 P-wave anisotropy parameters from 3D vertical seismic profile with distributed acoustic sensors and
671 geophones for seismic imaging in the CO2CRC Otway Project. Geophys Prospect 69, 842-855.
672 Popik, S., Pevzner, R., Tertyshnikov, K., Popik, D., Urosevic, M., Shulakova, V., Glubokovskikh, S.,
673 Gurevich, B., 2020. 4D surface seismic monitoring the evolution of a small CO2 plume during and after
674 injection: CO2CRC Otway Project study. Exploration Geophysics, 1-11.
675 Popik, S., Popik, D., Pevzner, R., 2019. Effect of Density of Seismic Sources on the Quality of the 4D
676 Seismic Data, 81th EAGE Conference & Exhibition 2019. EAGE, London, UK, p. Th_R09_04.
677 Qin, Z., Urosevic, M., Pevzner, R., 2020. Distributed Acoustic Sensing Technique for Seismic while
678 Drilling: Stage 3 of the CO2CRC Otway Project Case Study, EAGE Workshop on Fiber Optic Sensing for
679 Energy Applications in Asia Pacific, Kuala-Lumpur, Malaysia, pp. 1-5.
680 Schuster, G.T., 2009. Seismic Interferometry. Cambridge University Press, Cambridge.
681 Sidenko, E., Pevzner, R., Bona, A., Tertyshnikov, K., 2019. Seismic Interferometry Using Walkaway DAS
682 VSP Data: CO2CRC Otway Project Feasibility Study, 81th EAGE Conference & Exhibition 2019. EAGE,
683 London, UK, p. Tu_P05_02.
684 Spackman, T.W., 2019. Novel orbital seismic sources at a CO2 storage monitoring site, Newell County,
685 Alberta. University of Calgary, Calgary, Alberta, p. 113.
686 Storen, R., Corrigan, N., 2020. COVID-19: a chronology of state and territory government
687 announcements (up until 30 June 2020).
688 Tertyshnikov, K., Bergery, G., Freifeld, B., Pevzner, R., 2020. Seasonal Effects on DAS using Buried
689 Helically Wound Cables, EAGE Workshop on Fiber Optic Sensing for Energy Applications in Asia Pacific,
690 Kuala-Lumpur, Malaysia, p. S4_P7.
691 Tertyshnikov, K., Pevzner, R., Freifeld, B., Ricard, L., Avijegon, A., 2019a. DAS VSP for Characterisation
692 and Monitoring of the CO2 Shallow Release Site: CSIRO In-Situ Laboratory Case Study, Fifth EAGE
693 Workshop on Borehole Geophysics, The Hauge, pp. 1-5.

694 Tertyshnikov, K., Pevzner, R., Freifeld, B., Ricard, L., Avijegon, A., 2019b. Watching the leakage: DAS
695 seismic monitoring of the shallow CO2 controlled-release experiment at the South West Hub In-situ
696 Laboratory, SEG Technical Program Expanded Abstracts 2019, pp. 4888-4892.
697 White, D., Harris, K., Roach, L.A.N., Robertson, M., 2019. 7 years of 4D seismic monitoring at the
698 Aquistore CO2 storage site, Saskatchewan, Canada, SEG Technical Program Expanded Abstracts 2019,
699 pp. 4918-4922.
700 Yavuz, S., Isaenkov, R., Pevzner, R., Tertyshnikov, K., Yurikov, A., Correa, J., Wood, T., Freifeld, B., 2020.
701 Processing of Continuous Vertical Seismic Profile Data Acquired with Distributed Acoustic Sensors and
702 Surface Orbital Vibrators. 2020, 1-5.
703 Yurikov, A., Tertyshnikov, K., Isaenkov, R., Sidenko, E., Yavuz, S., Glubokovskikh, S., Barraclough, P.,
704 Gurevich, B., Pevzner, R., 2020. Multiwell 3D VSP with Fibre Optics for Monitoring of CO2 Injection,
705 EAGE Workshop on Fiber Optic Sensing for Energy Applications in Asia Pacific, Kuala-Lumpur, Malaysia,
706 pp. 1-5.
707 Zwartjes, P.M., Barker, T.B., Hornman, J.C., Przybysz-Jarnut, J., 2015. Quantitative Interpretation of
708 Nine Months of Daily SeisMovie™ Data to Monitor Steam Injection at Schoonebeek, 77th EAGE
709 Conference and Exhibition 2015, Madrid, Spain, pp. 1-5.
710